Effect of Thermal History on the Rheological Behavior of Thermoplastic Polyurethanes

Pil Joong Yoon and Chang Dae Han*

Department of Polymer Engineering, The University of Akron, Akron, Ohio 44325-0301

Received October 19, 1999; Revised Manuscript Received January 20, 2000

ABSTRACT: The effect of thermal history on the rheological behavior of ester- and ether-based commercial thermoplastic polyurethanes (TPUs) was investigated. ^{1}H and ^{13}C nuclear magnetic resonance (NMR) spectroscopy indicated that the ester-based TPU consisted of 4,4′-diphenylmethane diisocyanate (MDI) and butanediol (BDO) as hard segments and poly(tetramethylene adipate) as soft segments, and the ether-based TPU consisted of MDI−BDO as hard segments and poly(oxytetramethylene) as soft segments. The dynamic storage and loss moduli (G' and G'') of specimens, which had been prepared by injection molding at different temperatures, were monitored at a fixed angular frequency during isothermal annealing. It was found that injection molding temperature employed for specimen preparation had a profound influence on the variations of G' and G'' with time observed during isothermal annealing. Measurements were taken of the N−H stretching absorption bands in the Fourier transform infrared (FTIR) spectra during isothermal annealing at 170 °C for specimens prepared by injection molding at different temperatures. The analysis of FTIR spectra indicated that variations of hydrogen bonding with time during isothermal annealing resemble very much variations of G' with time during isothermal annealing. Isochronal dynamic temperature sweep experiments indicated that the TPUs exhibited hysteresis effect in the heating and cooling processes. It is concluded that the microphase separation transition or order−disorder transition in TPU cannot be determined from the isochronal dynamic temperature sweep experiment. It was observed that plots of log G' versus log G'' varied with temperature over the entire range of temperatures (110−190 °C) investigated, suggesting that the morphological state of the TPU specimens varied with temperature. Little evidence was found from ^{1}H and ^{13}C NMR spectroscopy that exchange reactions took place in the TPU specimens during isothermal annealing at elevated temperatures.

1. Introduction

During the past decades, thermoplastic polyurethane (TPU) has received considerable attention from both the scientific and industrial communities.[1−3] Applications of TPUs include automotive exterior body panels, medical implants such as the artificial heart, membranes, ski boots, and flexible tubing. TPU consists of hard and soft segments: hard segments are composed of diisocyanate (e.g., 4,4′-diphenylmethane diisocyanate (MDI)) and short-chain diols (e.g., butanediol (BDO)) as a chain extender that form a crystalline phase at a service temperature, while soft segments are composed of long-chain diols (e.g., poly(tetramethylene adipate (PTMA); poly(oxytetramethylene (POTM)) which control low-temperature properties. The soft segments form a flexible matrix between the hard domains. Often, TPUs are referred to as multiblock copolymers. To fully understand relationships between chemical structure and morphology and between chemical structure and physical properties of TPU, a complete characterization of the materials must be conducted. The physical and mechanical properties of TPU depend, among many factors, on (i) the composition of soft and hard segments, (ii) the lengths of soft and hard segments and the sequence of length distribution, (iii) anomalous linkages (branching, cross-linking), and (iv) molecular weight.

In some TPUs, the hard segments are crystalline, and crystallinity is part of the driving force leading to phase separation. The thermodynamic incompatibility between the urethane and polyol blocks is also part of the driving force leading to phase separation. The phase separation in TPU gives rise to relatively high modulus and high extensibility at room temperature. The hard segments act as physical cross-links between the flexible chains, and thus, the crystalline structure has great influence on the mechanical properties of TPU. At temperatures above the melting point of the hard segments, TPU forms mixed phases, while upon cooling below the melting point of the hard segments, its original structure is recovered. Some of the factors affecting the morphology and consequently the rheological behavior of TPUs include the chemical structures of hard and soft segments, the volume fraction of hard segments, hydrogen bonding, molecular weight, and thermal history.

In the past, much effort was spent on investigating thermal transitions in TPU by differential scanning calorimetry (DSC).[4−14] There is an abundance of experimental evidence that multiple thermal transitions take place during heating or cooling of TPU, suggesting that more than one form of crystals may be present in TPU. The situation becomes more complicated when the thermal history of a specimen greatly influences the morphology of a specimen. The thermal transitions in TPU reported in the literature may be summarized as follows: (i) a glass transition of either the hard or soft segments, (ii) an endotherm of the hard segments attributable to annealing, and (iii) endotherm associated with the long-range order of crystalline portions of either the soft or hard segments. In general, three endotherms associated with the hard segments are observed: (i) at 60−80 °C (endotherm I), (ii) at 120−180 °C (endotherm II), and (iii) at temperatures above 200 °C (endotherm III). The origin of the multiple endotherms in TPU is generally believed to be associated with different morphologies of the hard segments. These endotherms are very sensitive to the initial conditions (i.e., thermal and

10.1021/ma991741r CCC: $19.00
Published on Web 03/03/2000

processing histories) and annealing conditions. At present the morphological origin of multiple endotherms observed in TPU is not well understood.

TPUs are known to undergo a high degree of hydrogen bonding (i) between urethanes, (ii) between ester-based soft segment and urethane, and (iii) between ether-based soft segment and urethane. These various types of hydrogen bonding are also known to depend on temperature.[15−19] The formation of hydrogen bond in a TPU is complicated by phase intermixing[16] and dissociation−reorganization processes.[18]

To our great surprise, there are very few papers[20] reporting on the rheological behavior of TPUs, although there are some papers[21−23] reporting on the effect of thermal history of liquid-crystalline TPUs. In view of the fact that the mesogenic groups in a thermotropic liquid-crystalline polymer (TLCP) are primarily responsible for the observed thermal history effect on its rheological behavior,[24−27] it is not clear as to how much the mesogenic structure present in liquid-crystalline TPUs played a role in the observed thermal history effect on its rheological behavior.[21−23] We are not aware of any paper reporting on the effect of thermal history on the rheological behavior of TPUs. In view of the fact that TPUs have complex chemical structures and that the hard and soft segments in a TPU may intermix at elevated temperatures, it is not difficult to imagine that the rheological behavior of TPU would be very complicated.

Very recently we investigated the rheological behavior of ester- and ether-based commercial TPUs, putting emphasis on the effect of thermal history. Specifically, using a rotational-type rheometer with a parallel-plate fixture in oscillatory mode, we monitored, during isothermal annealing, variations of dynamic storage and loss moduli (G' and G'') with time of a specimen, which had been prepared by injection molding at different temperatures. We observed hysteresis effect from isochronal dynamic temperature sweep experiments in the heating and cooling processes. To offer explanations on the experimentally observed time evolution of G' and G'' of TPU during isothermal annealing, we investigated (i) the possibility, via DSC, of thermal transitions that might have occurred during isothermal annealing, (ii) the extent of hydrogen bonding, via in situ FTIR spectroscopy at elevated temperatures, that might have been formed during isothermal annealing, and (iii) the possibility of exchange reactions, via ^{1}H and ^{13}C nuclear magnetic resonance (NMR) spectroscopy, that might have occurred during isothermal annealing. In this paper we report the highlights of our findings.

2. Experimental Section

2.1. Materials and Sample Preparation. We used three grades of commercial TPU (Estane 5701, Estane 5707, and Estane 5714, BFGoodrich). Table 1 gives sample codes and the chemical structures of the TPUs determined in this study using ^{1}H and ^{13}C NMR spectroscopy. We found that ES01 and ES02 are ester-based TPUs and ET01 is an ether-based TPU. We have confirmed via NMR spectroscopy that ester-based ES01 and ES02 do not contain any fillers or additives, but ether-based ET01 contains ca. 4 wt % calcium stearate as an additive.

Specimens for rheological investigation were prepared using the procedures described below. As-received TPUs were dried in a vacuum oven at 70 °C for 48 h to eliminate moisture trapped in the materials. Annealing was carried out in a vacuum oven using dry nitrogen gas. Specimens of dumbbell shape were prepared using a Boy 15 injection molding machine at 180, 190, 200, 210, or 220 °C. The holding time was 2 min, and injection pressure was 103 MPa (1500 psi). The mold temperature was maintained at 40 °C. Also, disks of ca. 1.5 mm thick were prepared by compression molding at 138 MPa (2000 psi) at 180, 200, or 220 °C for 15−20 min and subsequently cooled quickly to room temperature using dry ice. Also, specimens were cooled slowly to room temperature at a rate of ca. 3 °C/min. All specimens prepared from injection molding were stored at − 24 °C in a refrigerator. Before rheological measurements, specimens were dried at 70 °C for 8 h in a vacuum oven to ensure that they were free from moisture.

Table 1. Compositions of the As-Received TPUs Determined by NMR Spectroscopy

	hard segment		soft segment	
sample code	MDI[d] (mol %)	BDO[e] (mol %)	TMO[f] (mol %)	AA[g] (mol %)
^{1}H NMR spectra				
ES01[a]	15	13	36	36
ES02[b]	18	16	33	33
ET01[c]	12	11	77	
^{13}C NMR spectra				
ES01[a]	16	11	36.5	36.5
ES02[b]	19	14	33.5	33.5
ET01[c]	12	9	79	

[a] MDI/BDO/PTMA (ester-based TPU). [b] MDI/BDO/PTMA (ester-based TPU). [c] MDI/BDO/POTM (ether-based TPU). [d] 4,4′-Diphenylmethane diisocynate. [e] 1,4-Butanediol. [f] Tetramethylene oxide. [g] Adipic acid.

2.2. Gel Permeation Chromatography (GPC). Molecular weight and molecular weight distribution were measured using a GPC equipped with a Waters 500 pump, three different columns, and a refractive index detector. Polystyrenes with different molecular weights were used as standards. The mobile phase was tetrahydrofuran (THF) at a rate of 1.0 mL/min, and the column temperature was maintained at 35 °C. All samples were prepared in THF at a concentration of 0.1% (w/v).

2.3. Differential Scanning Calorimetry (DSC). Thermal transitions in a specimen were determined using DSC. DSC measurements were conducted on a Perkin-Elmer DSC-7 equipped with an ice−water cooling system, under a nitrogen atmosphere, at a heating rate of 20 °C/min. Sample size used was 10−15 mg. Indium was used to calibrate the DSC cell constant.

2.4. Rheological Measurement. A Rheometrics mechanical spectrometer (Rheometrics Scientific, model RMS 800) was used in the oscillatory mode with parallel plate fixtures (25 mm diameter) and also in the steady-state shear mode with cone-and-plate fixtures (25 mm diameter plate and 5° cone angle). Dynamic storage modulus (G') and dynamic loss modulus (G'') were measured as functions of angular frequency (ω) ranging from 0.0178 to 56.23 rad/s at various temperatures. The temperature control was accurate to within ±1 °C, and a fixed strain of 0.04 was used at a given temperature, to ensure that measurements were taken well within the linear viscoelastic range of the materials investigated. All rheological measurements were conducted under a nitrogen atmosphere in order to preclude oxidative degradation of the samples.

Dynamic temperature sweep experiments under isochronal conditions were conducted at various angular frequencies (ω) from 120 to 190 °C during heating and from 190 to 100 °C during cooling. Measurement at each temperature took about 10 min. The temperature protocol of a specimen was as follows. First a specimen was placed in the parallel-plate fixture of the rheometer that had been heated to 180 °C and held there for 2 min in order to prevent slippage of specimen in the parallel plates, and then the specimen was cooled to about 70 °C, which took about 30 min, and then heated again to 120 °C. The preheating time at 120 °C was 20 min. A dynamic temperature sweep experiment was conducted using either the same specimen during both the heating and cooling processes or a fresh specimen for heating and cooling.

2.5. Fourier Transform Infrared Spectroscopy (FTIR). FTIR experiments were performed in order to determine the extent of hydrogen bonding in a TPU specimen during isothermal annealing at elevated temperatures, the results of which will be presented later in this paper. For the experiment, films suitable for spectroscopic studies were prepared by directly casting 2% (w/v) solution in THF on the KBr salt plate. It was slowly dried for 24 h in a fume hood until most of the solvent evaporated and then dried at 70 °C for a few days in a vacuum oven. Samples were then stored in a desiccator until used. FTIR spectra were obtained using a Perkin-Elmer spectrometer (model 16PC FTIR). Spectral resolution was maintained at 2 cm^{-1}. Dry nitrogen gas was used to purge the sample compartment in order to reduce the interference of water and carbon dioxide in the spectrum.

2.6. Nuclear Magnetic Resonance Spectroscopy (NMR). ^1H NMR and ^{13}C NMR spectroscopic experiments were conducted to identify the chemical structures of as-received TPU samples and to investigate possible anomalous linkages that might have been formed during isothermal annealing at elevated temperatures. ^1H NMR spectra were recorded at 200 MHz on a Varian Gemini-200 spectrometer. TPU specimens were dried in a vacuum oven at 70 °C for 24 h. They were then examined as 4% w/v solutions (40 mg/mL) in deuterated dimethyl sulfoxide (DMSO) for ester-based TPU specimens (ES01 and ES02) and in a mixture of deuteriochloroform ($CDCl_3$)/DMSO (ca. 50:50 v/v) for ether-based TPU (ET01) specimen. Typically, 128 scans were accumulated to provide adequate sensitivity. ^{13}C NMR spectroscopy was performed by the gated decoupling method to remove the nuclear overhauser enhancement (NOE). At least 5000 scans were averaged to provide high signal-noise ratio. A TPU solution of ca. 20% w/v concentration (200 mg/mL) was prepared in DMSO and a mixture of DMSO and $CDCl_3$.

3. Results and Discussion

3.1. Rheological Behavior of TPUs. (a) Time Evolution of Dynamic Storage Modulus in TPU during Isothermal Annealing. To find out whether we could reproduce rheological measurements under isothermal conditions, we carried out a dynamic frequency sweep experiment under the temperature protocol, shown schematically, in the upper panel of Figure 1. The lower panel of Figure 1 gives logarithmic plots of complex viscosity $|\eta^*|$ versus angular frequency ω for ES02 under the predetermined temperature protocol described above, where values of $|\eta^*|$ were calculated from $|\eta^*| = [(G'/\omega)^2 + (G''/\omega)^2]^{1/2}$. As can be seen in Figure 1, the frequency dependence of $|\eta^*|$ in steps 1, 3, and 5 at 170 °C was *not* reproduced, while the frequency dependence of $|\eta^*|$ in steps 2 and 4 at 190 °C was almost reproduced. The experimental results indicate to us that the morphological state in step 1 was not reproduced in steps 3 and 5. The above observations suggest to us that the thermal history of a TPU specimen greatly influences its rheological behavior.

Having observed that the dynamic frequency sweep measurement was not reproducible within the time scale of the experiment, we decided to monitor time evolution of G' under isothermal conditions at a fixed value of $\omega = 0.562$ rad/s for a period of 2 h. Figure 2 describes the time evolution of G' for ES02 during isothermal annealing at 170, 180, and 190 °C, respectively. It can be seen in Figure 2 that the time evolution of G' differs at each measurement temperature, namely, (i) at 170 °C the value of G' decreased very slowly for the first 30 min and then increased slowly with time for the rest of the experiment that lasted for 90 min; (ii) at 180 °C the value of G' increased for the first 70 min and then tended to level off for the remaining period of annealing; and (iii) at 190 °C, initially the value of G' increased rapidly, then went through a maximum at ca. 40 min after annealing began, and then decreased slowly until it tended to level off at ca. 2 h after annealing began. Somewhat similar results, not presented here, were obtained for ES01. However, as can be seen in Figure 3, the time evolution of G' for ET01 is quite different from that for ES02 in that at all three annealing temperatures, 170, 180, and 190 °C, the value of G' slowly decreased after annealing began and then leveled off soon, remaining there for the rest of the entire annealing period. The initial decrease of G' observed in Figure 3 may be associated with a transient period that is necessary for achieving an equilibrium morphology. This difference in time evolution of G' between the ester-based ES02 (Figure 2) and ether-based ET01 (Figure 3) during isothermal annealing may be attributable to the differences in chemical structure between ES02 and ET01. Below we will elaborate

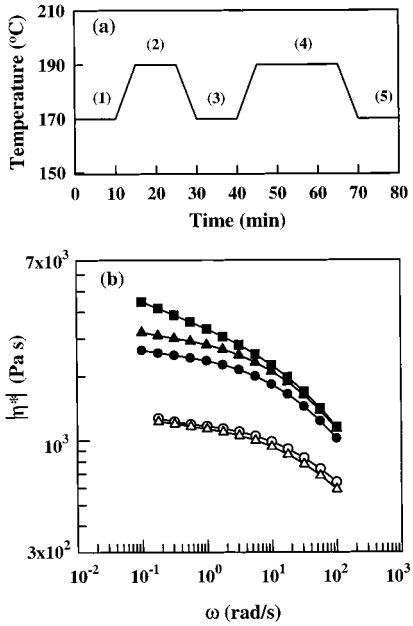

Figure 1. (a) Temperature protocol employed and (b) plots of log $|\eta^*|$ versus log ω for ES02 at various temperatures following the predetermined temperature protocol: (●) 170 °C (step 1); (○) 190 °C (step 2); (▲) 170 °C (step 3); (△) 190 °C (step 4); (■) 170 °C (step 5). A specimen prepared by compression molding at 180 °C was used for the entire experiment.

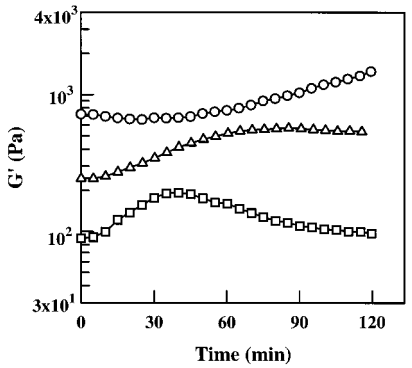

Figure 2. Variations of G' with time during isothermal annealing of ES02 at various temperatures: (○) 170 °C, (△) 180 °C, and (□) 190 °C. The specimens were prepared by injection molding at 180 °C, and G' was monitored at $\omega = 0.562$ rad/s.

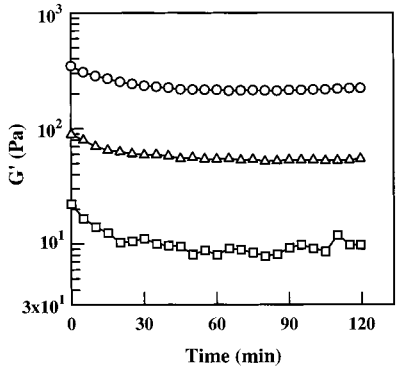

Figure 3. Variations of G' with time during isothermal annealing of ET01 at various temperatures: (○) 170 °C, (△) 180 °C, and (□) 190 °C. The specimens were prepared by injection molding at 180 °C, and G' was monitored at $\omega = 0.562$ rad/s.

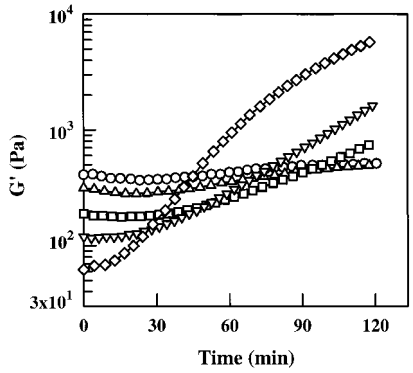

Figure 4. Effect of injection molding temperature employed for specimen preparation on the variations of G' with time during isothermal annealing of ES02 at 170 °C. The injection molding temperatures employed for specimen preparation are (○) 180 °C, (△) 190 °C, (□) 200 °C, (▽) 210 °C, and (◇) 220 °C. G' was monitored at $\omega = 0.237$ rad/s.

further on this speculation by presenting the results of other types of experiments performed in this study.

We also investigated how the injection molding temperature employed for specimen preparation might affect the time evolution of the rheological behavior of the TPUs. For this, we prepared specimens by injection molding at 180, 190, 200, 210, or 220 °C. Figure 4 describes the time evolution of G' for ES02 at a fixed angular frequency $\omega = 0.237$ rad/s after an injection-molded specimen was placed on the parallel-plate fixture of the rheometer under isothermal conditions at 170 °C for 2 h. It should be mentioned that a fresh specimen was used for each temperature. The following observations are worth noting: (i) for the specimens prepared by injection molding at 180 or 190 °C, the value of G' initially decreased moderately for ca. 30 min and then increased very slowly for the remaining 1.5 h; (ii) for the specimen prepared by injection molding at 200 or 210 °C the value of G' initially decreased very moderately for the first 30 min after annealing began and then increased for the remaining 1.5 h at a rate faster than that for the specimens injection molded at 180 or 190 °C; and (iii) for the specimen prepared by injection molding at 220 °C the value of G' started to increase rapidly from the beginning of annealing and then continued to increase at a fast rate, giving rise to the value of G' much greater than that for the specimens injection molded at 180, 190, 200, or 210 °C. When presenting the results of DSC later in this paper we will

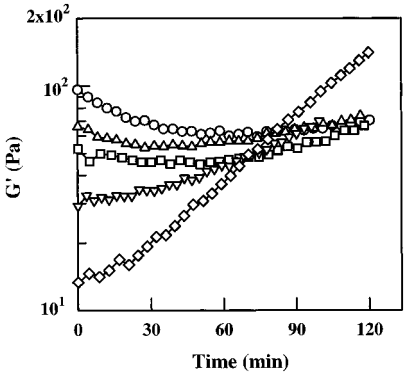

Figure 5. Effect of injection molding temperature employed for specimen preparation on the variations of G' with time during isothermal annealing of ET01 at 170 °C. The injection molding temperatures employed for specimen preparation are (○) 180 °C, (△) 190 °C, (□) 200 °C, (▽) 210 °C, and (◇) 220 °C. G' was monitored at $\omega = 0.237$ rad/s.

offer an explanation on the rapid increase of G' with time for the ET02 specimen injection molded at 220 °C during isothermal annealing at 170 °C for 2 h. We can conclude, on the basis of the observations made above, that the thermal history of a TPU specimen has a profound influence on its rheological behavior.

Interestingly, however, the time evolution of G' for ET01, given in Figure 5, is quite different from that for ES02 given in Figure 4. Namely, (i) for the specimen prepared by injection molding at 180 °C, the value of G' initially decreased at a moderate rate for ca. 30 min after annealing began and then leveled off and remained there for the subsequent 1.5 h; (ii) for the specimens prepared by injection molding at 190 and 200 °C the value of G' initially decreased very slowly and then leveled off followed by a slow increase at a moderate rate for the remaining 1.5 h; (iii) for the specimen prepared by injection molding at 210 °C the value of G' started to increase at a *moderate rate* at the beginning of annealing and continued to increase for the entire annealing period; and (iv) for the specimen prepared by injection molding at 220 °C the value of G' increased very rapidly from the beginning of annealing and continued to increase very rapidly. The above observations seem to indicate that the chemical structure, ester-based TPU versus ether-based TPU, plays an important role in variations of rheological behavior during isothermal annealing. Again, when presenting the results of DSC later in this paper we will offer an explanation on the rapid increase of G' with time for the ET01 specimen injection molded at 220 °C during isothermal annealing at 170 °C for 2 h.

(b) Variations of G' with Temperature during Isochronal Dynamic Temperature Sweep Experiment. Figure 6 describes variations of G' with temperature for ES01 during isochronal dynamic temperature sweep experiments at $\omega = 0.562$ rad/s in the heating and cooling processes. It can be seen from Figure 6 that the rheological behavior of ES01 in the heating process is quite different from that in the cooling process, indicating that the morphological state of ES01 in the heating process is quite different from that in the cooling process. Similar results, not presented here, were obtained for ES02 and ET01. The above observations reinforce once again that thermal history has a profound influence on the rheology of TPUs. As a matter of fact, earlier, similar hysteresis of rheological behavior has

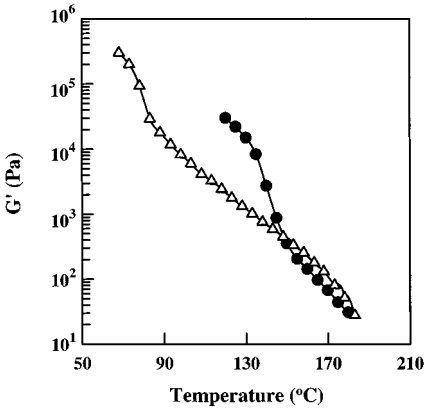

Figure 6. Variations of G' with temperature for ES01 in the heating (○) and cooling (●) processes at a rate of 0.5 °C/min during isochronal temperature sweep experiments at ω = 0.562 rad/s. A single specimen prepared by injection molding at 180 °C was employed for the entire experiment.

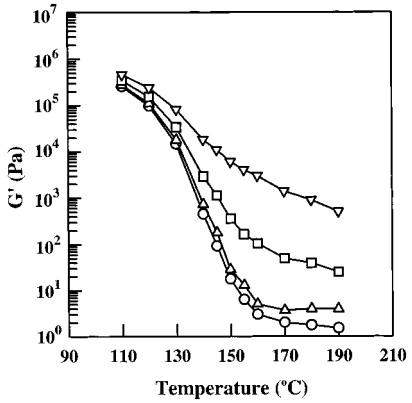

Figure 7. Variations of G' with temperature for ES01 in the heating process during the isochronal dynamic temperature sweep experiment at various angular frequencies: (○) 0.032 rad/s, (△) 0.1 rad/s, (□) 0.562 rad/s, and (▽) 5.62 rad/s. A single specimen prepared by injection molding at 180 °C was employed for the entire experiment.

been observed in main-chain TLCPs[28] and also in microphase-separated block copolymer.[29]

Figure 7 describes variations of G' with temperature for ES01, during heating, during isochronal dynamic temperature sweep experiments at various angular frequencies. It can be seen in Figure 7 that G' decreases gradually with increasing temperature and tends to level off at the lowest angular frequency employed, ω = 0.032 rad/s. Similar results, not presented here, were obtained for ES02 and ET01. It has amply been demonstrated in the literature[29] that the decreasing trend of G' with increasing temperature depends strongly on the angular frequencies applied.

In the past some investigators[30,31] made attempts to determine order−disorder transition (ODT) temperature (T_{ODT}) or microphase separation transition (MST) temperature (T_{MST}) in TPUs from isochronal dynamic temperature sweep experiments. Such attempts apparently were motivated by the rheological criterion for block copolymers in the literature,[32] which suggested that the temperature at which G' begins to drop precipitously from isochronal dynamic temperature sweep experiment be regarded as being T_{MST} or T_{ODT}. It should be mentioned that these two temperatures may be equated within the spirit of the Leibler theory.[33] Ryan et al.[30] attempted to determine the T_{ODT} of a TPU,

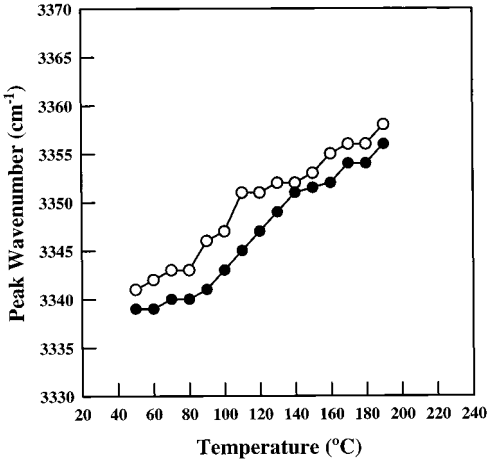

Figure 8. Temperature dependence of peak wavenumber of IR spectra in the N−H stretching region for ES01 in the heating (●) and cooling (○) processes at a rate of 0.5 °C/min. A fresh specimen prepared by injection molding at 180 °C was used for the heating and cooling processes.

which comprised hard segments formed from MDI and BDO and soft segments based on a poly(oxyethylene-*block*-oxypropylene) diol of molecular weight of 2300, from their isochronal dynamic temperature sweep experiment. However, their experimental data showed a gradual decrease in G' continuously from 140 to 180 °C and tended to level off at higher temperatures, very similar to that given in Figure 7. By observing the disappearance of a strong Bragg reflection at ca. 150 °C from the plots of intensity versus scattering vector obtained from small-angle X-ray scattering experiments, Ryan et al. concluded that their TPU underwent ODT at ca. 150 °C. In view of the fact that there was no sharp drop of G' at any particular temperature in their isochronal dynamic temperature sweep experiment, we are of the opinion that the determination of T_{ODT} from their experiment cannot be regarded as being conclusive.

Goddard and Cooper[31] also made an attempt to determine the T_{MST} of a TPU, which comprised hard segments formed from MDI and a diol as chain extender and soft segments based on POTM of molecular weight of 990, from isochronal dynamic temperature sweep experiments. Their data showed a gradual decrease of G' with increasing temperature from 60 to ca. 140 °C, the highest experimental temperature employed, very similar to Figure 7. In view of the fact that they could not identify any particular temperature at which G' dropped sharply from isochronal dynamic temperature sweep experiments and a homogeneous melt was not observed in their specimen over the entire range of temperatures tested, Goddard and Cooper[31] concluded that the determination of T_{MST} was very difficult. We are in agreement with Goddard and Cooper.[31]

The determination of MST or ODT in TPU is very difficult, if not impossible, from isochronal dynamic temperature sweep experiments for a number of reasons delineated below. Phase mixing between hard and soft segments continues above the melting point of hard segments. One such experimental evidence obtained in the present study is given below. Specifically, variations in peak wavenumber of N−H stretching bands in the FTIR spectra with temperature in the heating and cooling processes are given in Figure 8 for ES01. Similar results, not presented here, were obtained for ES02 and

ET01. In Figure 8 we observe a pronounced shift in peak wavenumber over the entire range of temperatures investigated. It should be mentioned that a broad shift in peak wavenumber of N−H stretching bands with temperature implies strong interactions between the soft and hard segments in the TPU specimen. This observation attests to the fact that phase mixing between the soft and hard segments continues in the temperature range tested up to 200 °C.

As will be shown below, hydrogen bonding takes place continuously in TPU, making the phase boundary between hard and soft segments blurred, although the extent of hydrogen bonding becomes weaker as the temperature is increased. Also, at elevated temperatures chemical reactions between isocyanate and active hydrogen in the urethane groups may take place, forming biuret or allophanate. The gradual decrease of G' with increasing temperature, instead of an abrupt decrease in G' at a particular temperature, observed in Figure 7, may be attributable in part to the hydrogen bonding taking place during rheological measurement. Thus, the gradual decrease of G' with increasing temperature observed in Figure 7 cannot be construed as the occurrence of ODT or MST.

TPUs can be regarded as being segmented multiblock copolymers with the segment lengths much shorter than those of AB- and ABA-type linear block copolymers. By taking into account all the factors listed above, we speculate that TPUs may easily lose long-range order at elevated temperatures barring chemical reactions or thermal degradation, thus transforming into short-range liquidlike order. If such a speculation is valid, the phase transition mechanism for TPU may be regarded as being very similar to that recently proposed by Sakamoto et al.[29] and Han et al.[34] for highly asymmetric sphere-forming block copolymers. According to these investigators, highly asymmetric block copolymers first undergo a lattice disordering/ordering transition (LDOT) at which the long-range order of microdomains is lost during heating, giving rise to a disordered arrangement of spheres with short-range liquidlike order (termed disordered spheres or micelles). Then, there is a demicellization/micellization transition (DMT) at which all microdomains disappear during heating and are transformed into the micelle-free homogeneous state in which the component polymers are mixed on a segmental level, and only thermally induced composition fluctuations may exist. They reported that the DMT temperature (T_{DMT}) is much higher than LDOT temperature (T_{LDOT}). It should be mentioned that T_{DMT} for highly asymmetric block copolymers corresponds to the conventional definition of T_{ODT} for symmetric or nearly symmetric block copolymers. If the phase transition mechanism for highly asymmetric block copolymers is applicable to TPUs, one may never be able to measure T_{DMT} for TPUs, if they undergo thermal degradation or chemical reactions before reaching T_{DMT}. Such a possibility is very high when using MDI-based TPUs, which have a rather high melting point.

(c) Temperature Dependence of log G' versus log G'' Plots for TPU. Figure 9 gives log G' versus log G'' plots for ES01 at various temperatures. Following Naumann et al.,[35] below log G' versus log G'' plots will be referred to as Han plots. We wish to point out that the Han plot has *no* relation whatsoever to the *empirical* Cole−Cole plot,[36] which gives a *temperature-depen*dent semicircle in rectangular coordinates, and that the Han plot has as its basis a molecular viscoelasticity theory for monodisperse homopolymers[37] and also for polydisperse homopolymers.[38] To maintain clarity, in Figure 9 we have divided the experimental data into two groups: (a) the upper panel gives Han plots which show a continuous *downward* shift with increasing temperature from 110 to 160 °C, and (b) the lower panel gives Han plots which show a continuous *upward* shift in the terminal region as the temperature is increased from 170 to 190 °C. It is of great interest to observe in Figure 9 that the Han plot having a slope much less than 2 at 110 °C moves downward with an increase in slope toward 2 as the temperature is increased from 110 to 170 °C, and then it starts to move upward as the temperature is increased further to 180 and 190 °C. Similar observations, not presented here, were made for ES02. Figure 10a gives Han plots for ET01 during heating from 140 to 190 °C, and Figure 10b gives Han plots for ET01 during cooling from 190 to 145 °C. Note in Figure 10 that during heating the Han plot moves *downward* and merges into a single curve with a slope in the terminal region still less than 2 at the highest experimental temperature employed, 190 °C, and during cooling the Han plot moves *upward* with decreasing temperature, giving rise to a slope progressively smaller with decreasing temperature. With reference to Figures 9 and 10, we observe an increase in G' with increasing temperature above a certain critical temperature. A real possibility exists that insoluble gels might have been formed during the dynamic frequency sweep experiments of ES01 at 180 and 190 °C, giving rise to an increase in G' in Figure 9.

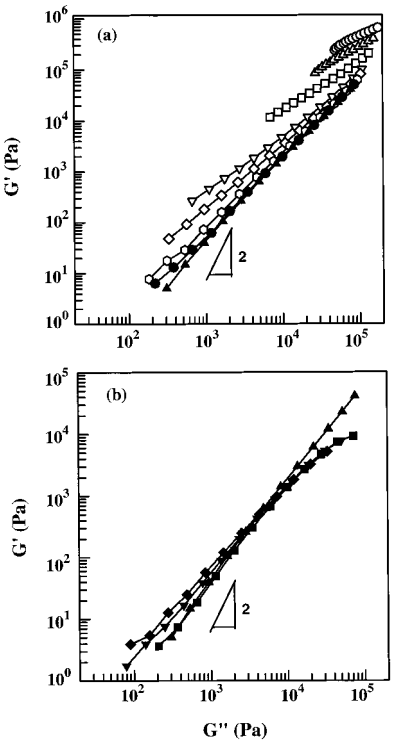

Figure 9. Han plots for ES01 in the heating process at various temperatures: (○) 110 °C, (△) 120 °C, (□) 130 °C, (▽) 140 °C, (◇) 145 °C, (⬠) 150 °C, (●) 155 °C, (▲) 160 °C, (■) 170 °C, (▼) 180 °C, and (◆) 190 °C. For the sake of clarity, the plots are divided into two parts: (a) the upper panel for temperatures from 110 to 160 °C and (b) the lower panel for temperatures from 160 to 190 °C. A single specimen prepared by injection molding at 180 °C was employed for the entire experiment.

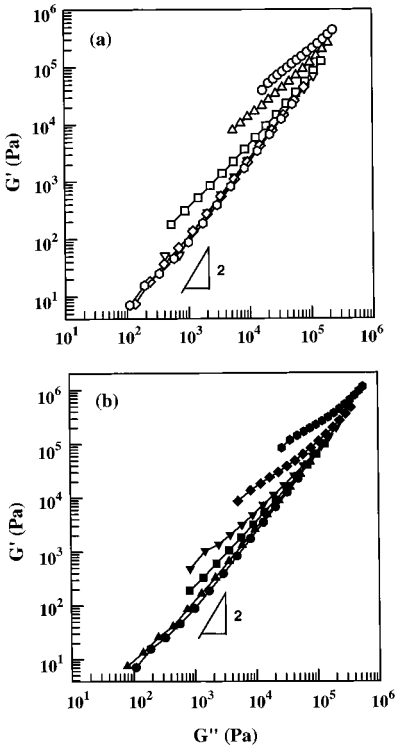

Figure 10. Han plots for ET01. (a) The upper panel describes the results for the heating process at various temperatures: (○) 140 °C, (△) 150 °C, (□) 160 °C, (▽) 170 °C, (◇) 180 °C, and (⬡) 190 °C. (b) The lower panel describes the results in the cooling process at various temperatures: (●) 190 °C, (▲) 180 °C, (■) 165 °C, (▼) 155 °C, and (◆) 145 °C. A single specimen prepared by injection molding at 180 °C was employed for the entire experiment.

The temperature dependence of the Han plot, observed in Figures 9 and 10, suggests that the morphology of the TPUs varies with temperature over the range of temperatures (110−190 °C) tested, because the homogeneous polymers are expected to exhibit temperature independence in Han plots.[37,38] It should be mentioned that the Han plot cannot determine how the morphology changes and what the new morphology might be, but only that it has changed as a function of temperature. We found that time−temperature superposition (TTS) failed to produce *reduced* (or *master*) plots for the three TPUs employed in this study. This is not surprising, because an application of TTS is not warranted to polymers whose morphology varies with temperature.[39]

3.2. Thermal Transitions in TPU during Isothermal Annealing. Figure 11 gives DSC traces of ES02 specimens that were annealed for 1 h in the rheometer at various temperatures indicated on the DSC trace. A fresh specimen was used for annealing at each temperature. The following observations are worth noting in Figure 11. The specimen without annealing shows two endotherms: endotherm I at 40−60 °C and endotherm II at 120−175 °C. As the annealing temperature is increased from 90 to 130 °C, endotherm I apparently merges into endotherm II, giving rise to a single endotherm with the peak position at ca. 140 °C. As the annealing temperature is increased further to 150 °C, a new broad endothermic peak starts to appear at 120−160 °C, while the intermediate peak is shifted to a high temperature (ca. 165 °C). When the annealing temperature is increased to 160 °C, both the lower and intermediate endothermic peaks are shifted to higher

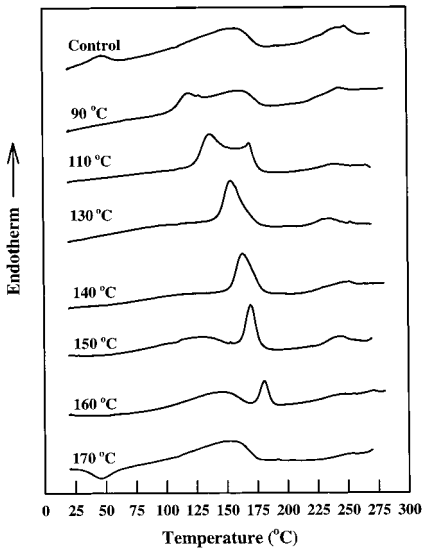

Figure 11. Effect of annealing temperature on thermal transitions, as determined by DSC, in ES02 specimens, which had been annealed for 1 h at a predetermined temperature indicated on the DSC trace. DSC runs were made at a heating rate of 20 °C/min, and an as-received specimen was used for each DSC run.

temperatures with the area under the intermediate peak becoming much smaller. However, at an annealing temperature of 170 °C, only a single endotherm peak is observed, drastically different from the DSC traces for specimens annealed at temperatures below 170 °C.

Figure 12a give DSC traces of ES02 specimens that were subjected to prolonged annealing (4−48 h) at various temperatures indicated on the DSC trace. From Figure 12a we observe that the prolonged annealing of as-received ES02 specimens at 90−150 °C does not produce a significant change in endothermic peak compared to the short-period annealing (see Figure 9). However, it is of interest to observe in Figure 12a that isothermal annealing at 170 °C for 4 h produced a new sharp endothermic peak at ca. 200 °C. Figure 12b gives DSC traces of ES02 specimens that were prepared by injection molding at 220 °C followed by isothermal annealing at 170 °C for various periods indicated on the DSC trace. Also given in Figure 12b, for comparison, is the DSC trace of an injection-molded specimen without annealing. Note that a fresh specimen was used for annealing for different time periods. From Figure 12b we observe that isothermal annealing of ES02 specimens at 170 °C for 30−120 min, after having been subjected to 220 °C, produced a new endothermic peak appearing at ca. 200 °C (endotherm III), which demonstrates the formation of a crystal-like structure. Not only does the position of endotherm III increase with annealing time, but so does the heat of fusion.

At this juncture we offer an explanation on the continuous increase in G' observed for the ES02 specimen (see Figure 4) and ET02 specimen (see Figure 5) during isothermal annealing at 170 °C after being injection molded at 220 °C. We learned that the specimen, which had been injection molded at 220 °C and then subjected to isothermal annealing at 170 °C for 2 h (see Figure 12b), was not dissolved in THF, but was dissolved in *N*,*N*′-dimethylformamide (DMF). This observation suggests to us that the rapid increase in G' observed in Figure 4 for ES02 and in Figure 5 for ET01 cannot be attributable to a possibility of the presence

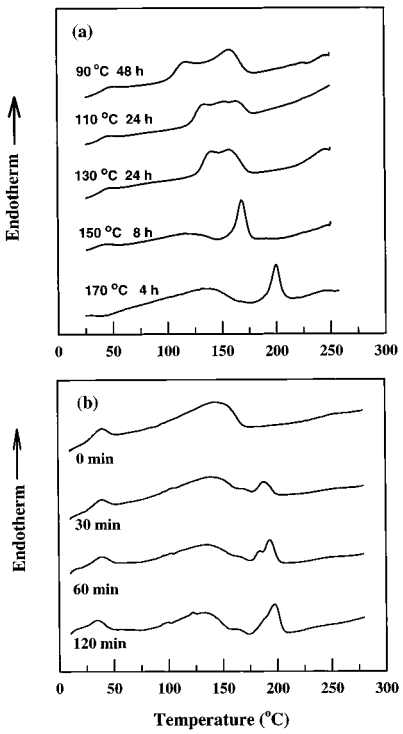

Figure 12. Effect of thermal history on thermal transitions, as determined by DSC, in ES02 specimens: (a) DSC trace of as-received ES02 specimens that were annealed at various temperatures and periods as indicated on the DSC trace and (b) DSC trace of the specimen that was injection molded at 220 °C followed by an isothermal annealing at 170 °C for various periods as indicated on the DSC trace. A fresh specimen was used for each DSC run at a heating rate of 20 °C/min.

of a cross-linked material in the specimen. Notice in Figure 12b that the endothermic peak at ca. 200 °C disappeared as the temperature was increased further during DSC scanning, indicating that the appearance of an endothermic peak at 200 °C in Figure 12b signifies the melting of high-temperature melting crystals that were formed during isothermal annealing. If a cross-linked material were formed during isothermal annealing, it would not melt away at 200 °C.

Further, we carried out DSC experiments on specimens before and after being subjected to oscillatory shear flow. Figure 13 gives DSC traces of ES02 specimens that were subjected to oscillatory shear flow at $\omega = 0.562$ rad/s for 2 h at 170, 180, and 190 °C. In other words, the specimens used for the DSC measurements were taken from the rheometer after annealing for 2 h while oscillatory shear flow was applied. It is interesting to observe in Figure 13 that annealing at different temperatures has produced little difference in thermal transition in ES02. From this observation we conclude that DSC is not sensitive enough to explain the physical origin of the time evolution of G' during isothermal annealing presented in Figures 2−5.

3.3. Hydrogen Bonding in TPU during Isothermal Annealing. To identify the absorption band in the TPU specimens employed in this study, we recorded IR spectra at room temperature in the range 500−3700 cm^{-1} as shown in Figure 14a for ES02 and in Figure 14b for ET01. Cooper and co-workers.[16,40] summarized band assignments for the N−H region and the carbonyl region. The inset of Figure 14a describes N−H stretching of ES02 from 3150 to 3500 cm^{-1}, and the inset of

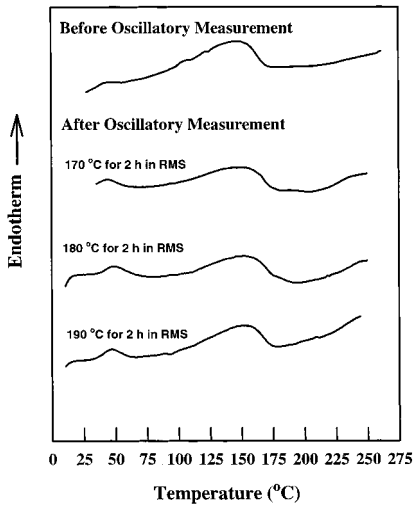

Figure 13. DSC traces for ES02 specimens before and after being subjected to oscillatory shear flow at $\omega = 0.562$ rad/s for 2 h at different temperatures, 170, 180, and 190 °C.

Figure 14b describes carbonyl stretching of ET01 from 1650 to 1800 cm^{-1}. The absorption bands at 2857 and 2960 cm^{-1} in Figure 14a are associated with symmetric and asymmetric CH_2 stretching vibrations, respectively, of the aliphatic CH_2 groups in ester-based ES02. In the case of ether-based ET01 given in Figure 14b, the absorption bands of CH_2 stretching vibrations appear at 2857 cm^{-1} (symmetric stretching) and 2940 cm^{-1} (asymmetric stretching). The area of these absorption bands was used to correct the variation in film thickness. The N−H absorption band of ES02 in the inset of Figure 14a is composed of at least four contributions. (i) The IR bands at 3440 and 3337 cm^{-1} are assigned to the N−H stretching modes of free and hydrogen-bonded N−H groups, respectively. (ii) The IR band at ca. 3120 cm^{-1} is attributed to an overtone of the C−N−H stretching−bending band at 1530 cm^{-1}. (iii) The weak shoulder at 3190 cm^{-1} is assigned to cis−trans isomerism of hydrogen-bonded N−H groups in the O═C−N−H structure. In the inset of Figure 14b, the carbonyl absorption band of ET01 is split distinctly into two peaks, one at 1732 cm^{-1} and the other at 1702 cm^{-1}, which are attributed to free and hydrogen-bonded carbonyl groups, respectively. In an ether-based TPU, the carbonyl groups exist only in the hard segments. Therefore, the relative absorbances of the two carbonyl peaks should serve as an index of the degree to which this group participates in the hydrogen bonding. The details of the procedure employed to determine the extent of hydrogen bonding in our TPU specimens during isothermal annealing are given in the literature.[16,19,40−43]

To investigate the effect, if any, of hydrogen bonding on the variations of G' with time during isothermal annealing presented in Figures 2−5, we carried out IR measurements during isothermal annealing at various temperatures by use of a spectrometer equipped with a hot plate. Figure 15 shows variations of N−H stretching bands of ES02 with increasing temperature from 30 to 250 °C in the spectrometer. In Figure 15 we make the following observations: (i) at 30 °C, most of the N−H groups are hydrogen-bonded as indicated by the large peak at about 3337 cm^{-1} with a very small shoulder at 3440 cm^{-1}, and (ii) with increasing temperature, the intensity of the free N−H band increases at the expense of the hydrogen-bonded N−H band and the peak of the

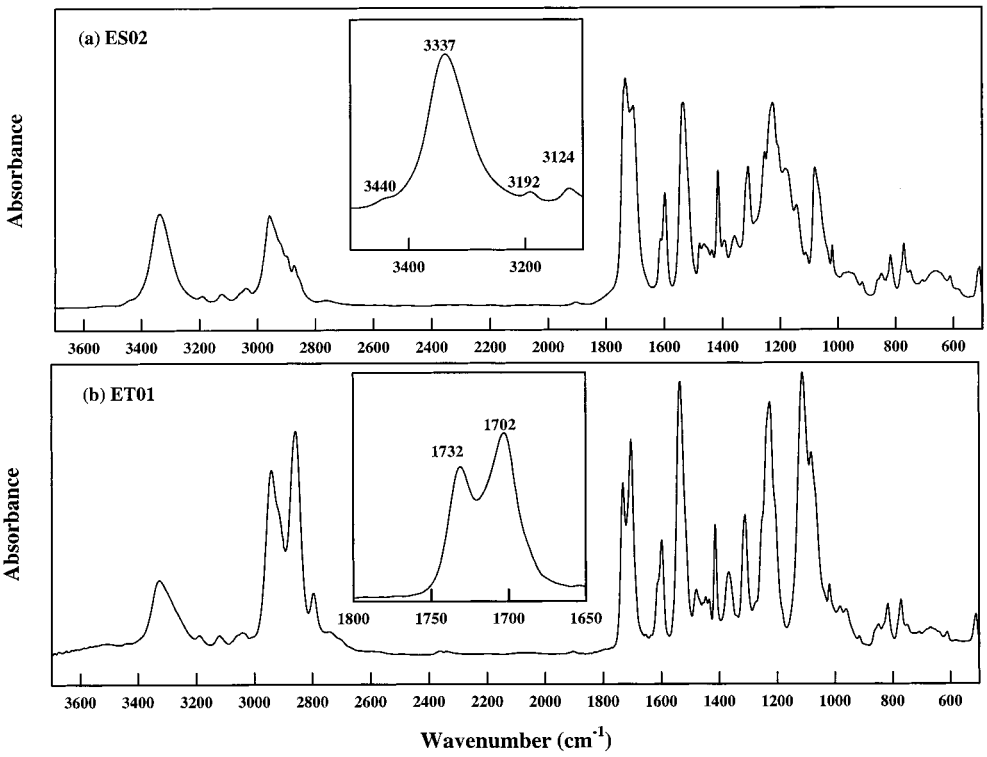

Figure 14. FTIR spectra of (a) as-received ES02 and (b) as-received ET01 at room temperature.

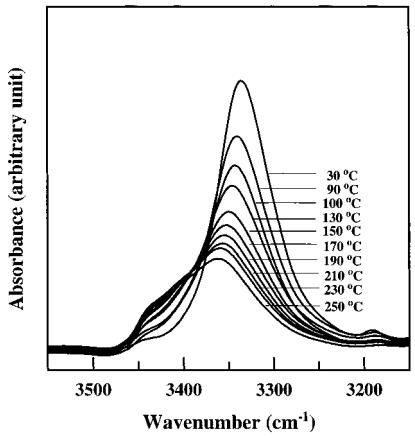

Figure 15. FTIR spectra in the N−H stretching region for as-received ES02 at various temperatures indicated on the IR spectra. The resolution was 2 cm^{-1}.

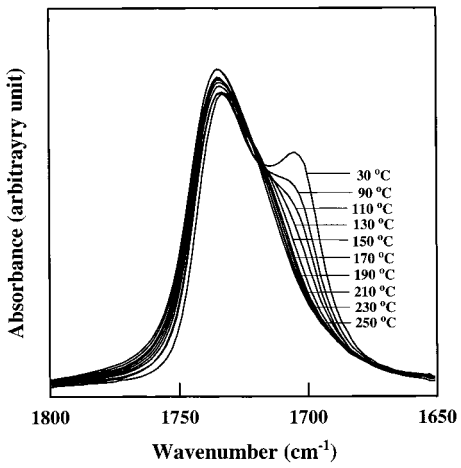

Figure 16. FTIR spectra in the C═O stretching region for as-received ES02 at various temperatures indicated on the IR spectra. The resolution was 2 cm^{-1}.

N−H band is shifted toward larger wavenumbers. Figure 16 gives the carbonyl absorption band in the IR spectra, showing distinct peaks that correspond to the free and the hydrogen-bonded groups in ES02 at 30 °C. As the temperature increased, the absorption intensities of carbonyl peaks increased. The fact that the positions of both the hydrogen-bonded N−H and carbonyl absorption are shifted to higher frequency with increasing temperature, as can be seen in Figures 15 and 16, indicates that the strength of hydrogen bonding is weakened with increasing temperature. However, without knowledge of the temperature dependence of the absorptivity coefficient, we cannot conclude whether the concentrations of free N−H and carbonyl groups increase with increasing temperature. Note that the absorption coefficient represents an average value of the strengths of functional groups (free N−H groups, hydrogen-bonded N−H groups, etc.)

Figure 17 gives the temperature dependence of IR spectra in the N═C═O stretching region for ES02, showing that the N═C═O band appears at temperatures above 190 °C and the area under the N═C═O absorbance peak (i.e., the concentration of N═C═O) increases with increasing temperature. The formation of free N═C═O at temperatures above 190 °C may be related to the thermal degradation of TPU by chain scission at the junction points of MDI and polyol and to subsequent secondary chemical reactions. The extent of thermal degradation was determined via GPC from the measurement of weight-average molecular weight (M_w) of specimens. Table 2 gives the effect of injection molding temperature on the M_w of TPU specimens, showing that an insignificant change in M_w (thus insignificant thermal degradation) occurred at temperatures up to 180 °C, and M_w decreased (thus measurable thermal degradation occurred) with increasing injection

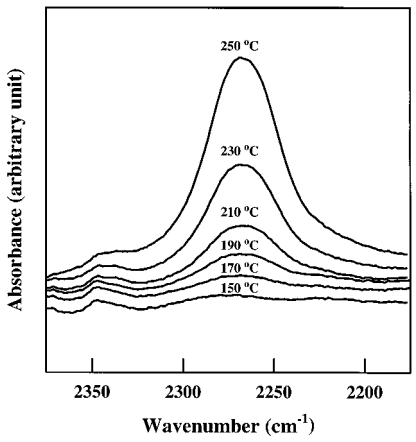

Figure 17. FTIR spectra in the N=C=O stretching region for as-received ES02 at various temperatures indicated on the IR spectra. The resolution was 2 cm^{-1}.

Table 2. Effect of Injection Molding Temperature on the Molecular Weight of the TPUs Investigated

sample code	processing temp (°C)[a]	M_w (g/mol)	M_w/M_n
ES01	virgin	124×10^3	1.68
	180	124×10^3	1.98
	200	80×10^3	1.62
	220	50×10^3	1.55
ES02	virgin	127×10^3	2.0
	180	114×10^3	1.8
	200	78×10^3	1.7
	200	66×10^3	1.6
ET01	virgin	170×10^3	1.9
	180	123×10^3	1.8
	200	93×10^3	1.8
	220	60×10^3	1.5

[a] Samples were prepared by injection molding at various temperatures.

Table 3. Effect of Annealing Temperature on the Molecular Weight of ES02[a]

annealing temp (°C)	annealing period (min)	M_w (g/mol)
170	0	112×10^3
	30	111×10^3
	60	109×10^3
	90	114×10^3
	120	115×10^3
180	0	109×10^3
	30	106×10^3
	60	106×10^3
	90	112×10^3
	120	113×10^3
190	0	102×10^3
	30	107×10^3
	60	*b*
	90	*b*
	120	*b*

[a] Each specimen was thermally equilibrated for 20 min at a predetermined temperature before isothermal annealing began. [b] Gels partially insoluble in THF were detected.

molding temperature. The readers are reminded that, during isothermal annealing, initially G' decreased as the molding temperature employed to prepare the specimens increased (see Figures 3−5). Table 3 describes the effect of annealing temperature on the M_w of ES02. In obtaining the results given in Table 3, a fresh specimen was placed in the DSC cell, where it received thermal treatment for a preset period. The following observations are worth noting in Table 3: (i) insignificant change in M_w (thus insignificant thermal degradation) occurred at 170 and 180 °C although there is a trend showing a slight decrease in M_w for the first

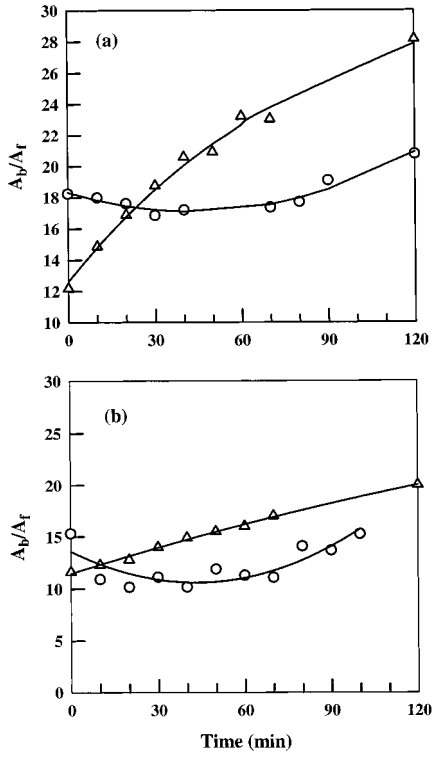

Figure 18. Variations of A_b/A_f ratio for the N−H stretching absorption bands in the FTIR spectra with time during isothermal annealing at 170 °C: (a) ES02 specimens prepared by injection molding at 180 °C (○) and 220 °C (△); (b) ET01 specimens prepared by injection molding at 180 °C (○) and 220 °C (△).

1 h followed by a slight increase in M_w thereafter, and (ii) insoluble gels in THF were formed in the solution of ES02 after annealing at 190 °C for 60−120 min.

Having observed in Figure 17 a significant increase in isocyanate groups for ES02 at temperatures above ca. 190 °C and in Table 3 evidence of the formation of insoluble gels in the solution of ES02 after annealing at 190 °C for 60−120 min, we now postulate that the rapid increase in G' observed during isothermal annealing at 180 and 190 °C (see Figure 2) may be attributable to a possibility of having formed biuret or allophanate via chemical reactions between isocyanate and active hydrogen in the urethane groups.

It is highly desirable to calculate the fraction of hydrogen-bonded N−H groups during isothermal annealing of TPU specimens in the FTIR spectrometer at various temperatures. This can be done when information on the molar absorptivity coefficient is available, as described in the Appendix. In the absence of such information on our TPU specimens in the literature and owing to the practical difficulties encountered, as described in the Appendix, with determining values of the molar absorption coefficient for our TPU specimens, in the present study we calculated A_b/A_f ratio at various temperatures from our IR spectra, where A_b is the area under the hydrogen-bonded absorbance peak and A_f is the area under the free hydrogen absorbance peak. Values of A_b and A_f were determined by curve-fitting the IR spectra recorded at various temperatures for each of the three TPUs employed.

Figure 18a describes variations of A_b/A_f ratio with annealing time, obtained during the in-situ FTIR measurements, for ES02 specimens that were prepared by injection molding at 180 and 220 °C. Similar results are

given in Figure 18b for ET01 specimens. It is of interest to observe in Figure 18 that the time evolution of the A_b/A_f ratio during isothermal annealing given in Figure 18 resembles very much the time evolution of G' during isothermal annealing given in Figures 4 and 5. On the basis of the above observations, we tentatively conclude that the time evolution of G' observed by oscillatory shear rheometry during isothermal annealing is related to the time evolution of the A_b/A_f ratio observed by FTIR spectroscopy during isothermal annealing. We speculate that both are the consequence of concomitant variations in morphology during isothermal annealing.

3.4. Exchange Reactions in TPU during Isothermal Annealing. It is well-established today that exchange reactions take place, for instance, in poly(ethylene terephthalate)/polycarbonate and poly(butylene terephthalate)/polycarbonate blends.[44,45] In view of the fact that the soft segments and urethane units in ester-based TPU have carbonyl groups, we felt that it was reasonable to speculate that exchange reactions in TPU might take place during the rheological measurements under isothermal conditions. We felt further that if this speculation were borne out to be correct, we would then be able to explain, at least in part, the variations of G' with time during isothermal annealing presented in Figures 2−5.

For the TPUs employed in this study, exchange reactions of ester units and urethane units might take place in the ester-based TPU (MDI/BDO/PTMA system), and exchange reactions of only urethane units might take place in the ether-based TPU (MDI/BDO/POTM system). In the past, high-resolution NMR spectroscopy was used to identify the chemical structures of various polyurethanes (PU),[46−55] indicating that ^{13}C NMR spectroscopy is much more useful than ^{1}H NMR spectroscopy in identifying the chemical structures of polyurethanes, because NH proton signals are rather sensitive to the environment (solvent, water, temperature, etc.). The assignments of ^{13}C NMR chemical shifts for PU are reported by several research groups,[46−49] and the assignments of ^{1}H NMR chemical shifts for PU are reported by Brame[54] and Okuto.[55] On the other hand, owing to the relaxation and nuclear Overhauser enhancement effects, a quantitative analysis of chemical composition in TPU is rather difficult using ^{13}C NMR spectra.

In the present study we obtained both ^{13}C and ^{1}H NMR spectra of our TPU specimens before and after being subjected to isothermal annealing. We could not discern measurable differences in the NMR spectra for specimens before and after isothermal annealing. We ascribe this finding to the fact that both the soft segments and the urethane units have four methylene units, making it very difficult to discern exchange reactions between the two.

4. Concluding Remarks

In this paper we have presented the results of our recent rheological investigation of three commercial TPUs in the molten state, showing that (i) the previous thermal history of a specimen (e.g., injection molding temperature used for sample preparation) has a profound influence on the rheological behavior of TPU, (ii) the dynamic viscoelastic properties of a TPU specimen, placed in the parallel-plate fixture of a rotational-type rheometer, varies with time during isothermal annealing, and (iii) TPU exhibits hysteresis effects during heating and cooling processes. To the best of our knowledge, such findings have never been reported in the literature.

In an effort to explain the seemingly complicated rheological behavior observed in the TPUs employed, we conducted additional experiments: (i) DSC to investigate whether thermal transitions might have occurred in TPU specimens during isothermal annealing, (ii) GPC to determine whether the molecular weight of a TPU specimen might have been changed by the injection molding temperatures employed for sample preparation, thermal degradation, or chemical reactions during isothermal annealing, (iii) in situ FTIR spectroscopy at elevated temperatures, simulating the thermal history that a specimen experienced during rheological measurement, to determine whether hydrogen bonding might have played a role in the observed variations of G' with time during isothermal annealing, and (iv) ^{1}H and ^{13}C NMR spectroscopy to determine whether exchange reactions might have played a role in the observed variations of G' with time during isothermal annealing by using specimens that had been subjected to the same thermal history as for rheological measurements. From such experiments we have reached the following conclusions. DSC was not sensitive enough to discern thermal transitions, if any, during isothermal annealing. At temperatures above ca. 190 °C for an extended annealing period, we found evidence for the formation of gels that could not be dissolved in THF, suggesting that chemical reactions took place at such high temperatures. FTIR spectra indicated that hydrogen bonding occurred during isothermal annealing, and the time evolution of the extent of hydrogen bonding showed a trend very similar to the time evolution of the dynamic storage modulus G' of a specimen during isothermal annealing in a rheometer. We could not discern any measurable evidence for exchange reactions, as determined by NMR spectra, that might have taken place during isothermal annealing, suggesting that exchange reactions cannot be responsible for the observed variations in G' with time during isothermal annealing. Thus, we tentatively conclude at the present time that the time evolution of G' during isothermal annealing may be attributable to the formation of hydrogen bonding.

Once we realize the fact that TPU is a structured fluid, like TLCP and microphase-separated block copolymer, the complex rheological behavior observed in this study is not surprising to us. Earlier, when investigating the rheological behavior of TLCP, Kim and Han[25] observed a time evolution of G' during isothermal annealing, very similar to that observed in the present study (see Figures 3−5). They also reported the hysteresis effect in TLCP during heating and cooling processes.[28] As a matter of fact, very recently the hysteresis effect was also observed in a microphase-separated block copolymer.[29]

There is, however, one very important difference between TPU and TLCP and between TPU and block copolymer, insofar as controlling the initial morphology of specimens before being subjected to rheological measurement. Specifically, Kim and Han[25] observed a continuous increase in G' during isothermal annealing of a TLCP in a rheometer. Subsequently, Han et al.[56] identified the origin of the time evolution of the rheological properties during isothermal annealing as being due to the continuous growth of crystals, which had been

Table 4. Curve-Fitting Results for C=O Stretching Region in the FTIR Spectra of ET01

	free C=O		disordered H-bonded C=O		ordered H-bonded C=O		
temp (°C)	freq (cm^{-1})	A_f	freq (cm^{-1})	A_{dr}[a]	freq (cm^{-1})	A_{or}[b]	A_T[c]
50	1732	9.3	1716	2.1	1703	10.0	21.4
70	1733	9.5	1716	3.1	1703	9.9	21.4
90	1734	9.9	1717	3.2	1703	8.4	21.5
110	1735	10.0	1717	4.5	1703	6.9	21.4
130	1736	10.0	1717	6.0	1703	5.5	21.5
150	1737	10.2	1717	6.4	1703	4.9	21.5
170	1737	11.4	1718	5.5	1703	4.7	21.6
190	1738	11.7	1719	5.2	1703	4.3	21.2
210	1738	11.7	1719	5.1	1703	4.2	21.0
230	1739	11.2	1719	5.0	1703	3.9	20.1

[a] $A_{dr}(T)$ is the area of disordered hydrogen-bonded carbonyl groups. [b] $A_{or}(T)$ is the area of ordered hydrogen-bonded carbonyl groups. [c] $A_T(T) = A_f + T_{dr}(T) + A_{or}(T)$.

formed via crystallization during isothermal annealing at temperatures below the melting point of high-temperature melting crystals. Kim and Han[25,26] demonstrated that the previous thermal history of a TLCP specimen can be erased by first heating a specimen above its clearing (or isotropization) temperature (T_{cl}) and holding it there for a while under a mild shearing and then cooling the specimen very slowly to a preset temperature in an anisotropic state. When dealing with glassy TLCPs, the problem becomes much less complicated, as shown by Chang and Han.[57] However, in the present study we could *not* erase the previous thermal history of a TPU specimen by heating the specimen above a certain critical temperature, because it undergoes either thermal degradation or chemical reaction(s) at temperatures above ca. 190 °C. In other words, there is no clearing temperature, so to speak, in TPUs. In dealing with glassy block copolymers (e.g., diene-based block copolymers with polystyrene), the problem is much simpler than the situation of TLCP in that there is no crystallization taking place in a specimen. However, one should be extremely careful with annealing a block copolymer specimen to attain an equilibrium morphology. This is particularly so when dealing with highly asymmetric block copolymer in composition. A recent study by Han et al.[34] showed that *highly asymmetric* block copolymers would require much longer annealing times than *symmetric* block copolymers to attain an equilibrium morphology. We hasten to point out that the situation will be different when dealing with semicrystalline block copolymers.

The similarity in rheological behavior between TPU and block copolymer on one hand and between TPU and TLCP on the other hand is not a coincidence, because the chains of TPU consist of segmented blocks characteristic of block copolymers on one hand and contain rather stiff molecules on the other hand. The polar nature of the urethane segments results in a strong mutual attraction, aggregation, and ordering into crystalline and paracrystalline domains in the mobile soft-segment matrix. The abundance of urethane hydrogen atoms, as well as carbonyl and ether oxygen partners, permits extensive hydrogen bonding among polymer chains, which apparently restricts the mobility of the urethane chain segments in the domains. Thus, one should expect that the rheological behavior of TPU would depend strongly on its morphological state, which in turn would strongly depend on thermal history. Owing to the very complicated nature of temperature-dependent morphology of TPU, at present it is not possible to explain completely the origin of the seemingly very complex rheological behavior presented above. What is urgently needed is simultaneous investigations of the morphology and the molecular conformations of TPU by mobilizing many characterization techniques, such as small-angle X-ray scattering, FTIR spectroscopy, transmission electron microscopy, dielectric spectroscopy, solid-state NMR spectroscopy, etc. In conclusion, we feel that we have only scratched the surface of the very complicated rheological behavior of TPU.

Appendix. Analysis of Hydrogen Bonding in TPU

From the N−H stretching absorption bands in the FTIR spectra for TPU, the fraction of hydrogen-bonded groups, X_{HB}, can be calculated from[16,41]

$$\frac{c_b}{c_o} = X_{HB} = \left\{1 + k\left[\frac{A_f(T)}{A_b(T)}\right]\right\}^{-1} \qquad \text{(A1)}$$

where c_b and c_o respectively are the concentration of hydrogen-bonded groups and the total concentration of hydrogen in the specimen, k is the ratio of absorptivity coefficient of the hydrogen-bonded N−H group and the absorptivity coefficient of the free N−H group, $A_f(T)$ is the area under the free hydrogen absorbance peak, and A_b is the area under the hydrogen-bonded absorbance peak. Note that k, $A_f(T)$, and $A_b(T)$ are known to depend on temperature. When values of $A_f(T)$ and $A_b(T)$ are determined from curve resolution procedures and k is determined experimentally, X_{HB} can be calculated from eq A1.

In the present study an iterative least-squares computer program was used to determine $A_f(T)$ and $A_b(T)$ from FTIR spectra by varying the frequency, the width at half-height, and the intensity of contributing bands. To calculate the fraction of hydrogen-bonded N−H or C=O groups, it is necessary to determine the value of k. It is known that k is dependent on temperature.[42] Coleman et al.[19] calculated the value of k of a polyurethane (having only hard segments) using the spectra obtained at varying temperatures ranging from 30 to 210 °C and found that k varied from ca. 5.4 to 2.9. Also, Goddard and Cooper[40] calculated the value of k of polyurethane ionomers.

In the present study the value of k was varied until the corrected total area under absorption bands, and the total absorption area at temperature T, $A_T(T)'$, was constant within errors over the temperature range investigated:

$$A_T(T)' = A_f(T) + A_b(T)' \qquad \text{(A2)}$$

where $A_b(T)' = A_b(T)/k$. Then, $A_T(T_1)' = A_T(T_2)'$ yields[19]

$$k = \frac{A_b(T_2) - A_b(T_1)}{A_f(T_1) - A_f(T_2)} \quad \text{(A3)}$$

A least-squares program enabled us to determine the value of k using eq A3. Table 4 gives, for illustration, curve-fitting results for the C═O stretching region of ET01 using the FTIR spectra obtained by varying the temperature from 50 to 230 °C. In Table 4 we used three Gaussian peaks to resolve the IR spectra. Using eq A3, the value of k was determined to be 1.74 for the C═O absorptions of ET01. However, it is not possible to calculate values of k from the C═O absorption bands of ES01 and ES02 since we must consider the contributions from C═O groups of soft segments. The C═O absorption bands of ester-based TPU consist of at least five peaks (three peaks from free, ordered, and disordered C═O groups from hard segments; two peaks from free and bonded C═O groups from soft segments). However, the second-derivative spectra of ester-based TPU gave three major spectral components, indicating that the absorption band could not be resolved to five contributing peaks.

References and Notes

(1) Saunders, J. H.; Frisch, K. C. *Polyurethane Chemistry and Technology, Part I*; Interscience: New York, 1962.
(2) Hepburn, C. *Polyurethane Elastomers*; Elsevier Applied Science: New York, 1992.
(3) Oertel, G., Ed. *Polyurethane Handbook*; Hanser: Munich, 1994.
(4) Sung, C. S. P.; Schneider, N. S. *Macromolecules* **1975**, *8*, 68.
(5) Sung, C. S. P.; Schneider, N. S. *Macromolecules* **1977**, *10*, 452.
(6) Sung, C. S. P.; Schneider, N. S. *J. Mater. Sci.* **1978**, *13*, 1689.
(7) Wilkes, G. L.; Bagrodia, S.; Humphries, W.; Wildnauer, R. *J. Polym. Sci., Polym. Lett.* **1975**, *13*, 321.
(8) Wilkes, G. L.; Wildnauer, R. *J. Appl. Phys.* **1975**, *46*, 4148.
(9) Kwei, T. K. *J. Appl. Polym. Sci.* **1982**, *27*, 2891.
(10) Hesketh, T. R.; Van Borgart, J. W. C.; Cooper, S. L. *Polym. Eng. Sci.* **1980**, *20*, 190.
(11) Seymour, R. W.; Cooper, S. L. *J. Polym. Sci., Polym. Lett.* **1971**, *9*, 689.
(12) Seymour, R. W.; Cooper, S. L. *Macromolecules* **1973**, *6*, 48.
(13) Koberstein, J. T.; Russell, T. P. *Macromolecules* **1986**, *19*, 714.
(14) Leung, L. M.; Koberstein, J. T. *Macromolecules* **1986**, *19*, 706.
(15) Seymour, R. W.; Estes, G. M.; Cooper, S. L. *Macromolecules* **1970**, *3*, 1579.
(16) Srichatrapimuk, V. W.; Cooper, S. L. *J. Macromol. Sci., Phys.* **1978**, *B15*, 267.
(17) Senich, G. A.; MacKnight, W. J. *Macromolecules* **1980**, *13*, 106.
(18) Jacques, C. H. M. In *Polymer Alloys*; Klempner, D., Frisch, K. C., Eds.; Plenum Press: New York, 1977; p 287.
(19) Coleman, M. M.; Lee, K. H.; Skrovanek, D. J.; Painter, P. C. *Macromolecules* **1986**, *19*, 2149.
(20) Velankar, S.; Cooper, S. L. *Macromolecules*, **1998**, *31*, 9181.
(21) Stenhouse, P. J.; Valles, E. M.; Kantor, S. W.; MacKnight, W. J. *Macromolecules* **1989**, *22*, 1467.
(22) Smyth, G.; Valles, E. M.; Pollack, S. K.; Grebowicz, J.; Stenhouse, P. J.; Hsu, S. L.; MacKnight, W. J. *Macromolecules* **1990**, *23*, 3389.
(23) Wedler, W.; Tang, W.; Winter, H. H.; MacKnight, W. J.; Farris, R. J. *Macromolecules* **1995**, *28*, 512.
(24) Lin, Y. G.; Winter, H. H. *Macromolecules* **1991**, *24*, 2877.
(25) Kim, S. S.; Han, C. D. *Macromolecules* **1993**, *26*, 3176.
(26) Kim, S. S.; Han, C. D. *J. Rheol.* **1993**, *37*, 847.
(27) Han, C. D.; Chang, S.; Kim, S. S. *Mol. Cryst. Liq. Cryst.* **1994**, *254*, 335.
(28) Kim, S. S.; Han, C. D. *Polymer* **1994**, *35*, 93.
(29) Sakamoto, N.; Hashimoto, T.; Han, C. D.; Kim, D.; Vaidya, N. Y. *Macromolecules* **1997**, *30*, 1621.
(30) Ryan, A. J.; Macosko, C. W.; Bras, W. *Macromolecules* **1992**, *25*, 6277.
(31) Goddard, R. J.; Cooper, S. L. *Macromolecules* **1995**, *28*, 1401.
(32) (a) Gouinlock, E. V.; Porter, R. S. *Polym. Eng. Sci.* **1977**, *17*, 535. (b) Chung, C. I.; Lin, M. I. *J. Polym. Sci., Polym. Phys. Ed.* **1978**, *16*, 545. (c) Widmaier, J. M.; Meyer, G. C. *J. Polym. Sci., Polym. Phys. Ed.* **1980**, *18*, 2217.
(33) Leibler, L. *Macromolecules* **1980**, *13*, 1602.
(34) Han, C. D.; Vaidya, N. Y.; Kim, D.; Shin, G.; Yamaguchi, D.; Hashimoto, T. Submitted to *Macromolecules*.
(35) Neumann, C.; Loveday, D. R.; Abetz, V.; Stadler, R. *Macromolecules* **1998**, *31*, 2493. These authors referred to the logarithmic plot of G' versus G'' as the Han plot.
(36) Cole, K. S.; Cole, R. H. *J. Chem. Phys.* **1941**, *9*, 341.
(37) Han, C. D.; Jhon, M. S. *J. Appl. Polym. Sci.* **1986**, *32*, 3809.
(38) Han, C. D.; Kim, J. K. *Macromolecules* **1989**, *22*, 4292.
(39) Han, C. D.; Kim, J. K. *Polymer* **1993**, *34*, 2533.
(40) Goddard, R. J.; Cooper, S. L. *Macromolecules* **1995**, *28*, 1390.
(41) Yang, M.; MacKnight, W. J. *J. Polym. Sci., Symp.* **1973**, *42*, 817.
(42) Coleman, M. M.; Graf, J. E.; Painter, P. C. *Specific Interactions and the Miscibility of Polymer Blends*; Technomic: Lancaster, PA, 1991.
(43) Yang, M. The Physical Properties of Polyurethanes. Doctoral Dissertation, University of Massachusetts, Amherst, MA, 1972.
(44) Devaux, J.; Goddard, P.; Mercier, S. P. *Polym. Eng. Sci.* **1982**, *22*, 229.
(45) Montaudo, G.; Puglisi, C.; Samperi, F. *Macromolecules* **1998**, *31*, 650 and references therein.
(46) Kaji, A.; Arimatsu, Y.; Murano, M. *J. Polym. Sci., Polym. Chem.* **1992**, *30*, 287.
(47) Ray, A. R.; Bhowmick, A. *J. Macromol. Sci., Chem.* **1991**, *A28*, 1009.
(48) Kaji, A.; Murano, M. *Polym. J.* **1990**, *22*, 1065.
(49) Delides, C.; Pethrick, R. A.; Cunliffe, A. V.; Klein, P. G. *Polymer* **1981**, *22*, 1205.
(50) Matthews, K. H.; McLennaghan, A.; Pethrick, R. A. *Br. Polym. J.* **1987**, *19*, 165.
(51) Chokki, Y. *Makromol. Chem.* **1974**, *175*, 3425.
(52) Chokki, Y.; Nakamitsu, M.; Sumi, M. *Makromol. Chem.* **1972**, *153*, 189.
(53) Suzuki, H.; Ono, H.; Hongo, T. *Makromol. Chem.* **1970**, *132*, 309.
(54) Brame, E. G.; Ferguson, R. C.; Thomas, G. J. *Anal. Chem.* **1967**, *39*, 517.
(55) Okuto, H. *Makromol. Chem.* **1966**, *98*, 148.
(56) Han, C. D.; Chang, S.; Kim, S. S. *Macromolecules* **1994**, *27*, 7699.
(57) Chang, S.; Han, C. D. *Macromolecules* **1997**, *30*, 1656.

MA991741R